TOXICOLOGICAL SCIENCES, 162(2), 2018, 548–558

doi: 10.1093/toxsci/kfx275
Advance Access Publication Date: December 1, 2017
Research Article

Dioxin-like PCB 126 Increases Systemic Inflammation and Accelerates Atherosclerosis in Lean LDL Receptor-Deficient Mice

Michael C. Petriello,[*,†,‡] J. Anthony Brandon,[*] Jessie Hoffman,[†,§] Chunyan Wang,[†,¶] Himi Tripathi,[||] Ahmed Abdel-Latif,[||] Xiang Ye,[|||] Xiangan Li,[|||] Liping Yang,[*] Eun Lee,[||||] Sony Soman,[*,†,‡] Jazmyne Barney,[†] Banrida Wahlang,[†] Bernhard Hennig,[†,¶] and Andrew J. Morris[*,†,‡,1]

[*]Division of Cardiovascular Medicine, College of Medicine and [†]Superfund Research Center, University of Kentucky, Lexington, Kentucky 40536; [‡]Lexington Veterans Affairs Medical Center, Lexington, Kentucky 40502; and [§]Department of Pharmacology and Nutritional Sciences, College of Medicine, [¶]Department of Animal and Food Sciences, College of Agriculture Food and Environment, [||]Gill Heart and Vascular Institute and Division of Cardiovascular Medicine, [|||]Department of Physiology, Saha Cardiovascular Research Center, and [||||]Department of Pathology and Laboratory Medicine, College of Medicine, University of Kentucky, Lexington, Kentucky 40536

[1]To whom correspondence should be addressed at Superfund Research Center, University of Kentucky, 900 S. Limestone Street, Lexington, KY 40536. Fax: (859) 257-1811. E-mail: a.j.morris@uky.edu.

ABSTRACT

Exposure to dioxins and related persistent organic pollutants likely contributes to cardiovascular disease (CVD) risk through multiple mechanisms including the induction of chronic inflammation. Epidemiological studies have shown that leaner individuals may be more susceptible to the detrimental effects of lipophilic toxicants because they lack large adipose tissue depots that can accumulate and sequester these pollutants. This phenomenon complicates efforts to study mechanisms of pollutant-accelerated atherosclerosis in experimental animal models where high-fat feeding and adipose expansion limit the bioavailability of lipophilic pollutants. Here, we investigated whether a model dioxin-like pollutant, PCB 126, could increase inflammation and accelerate atherosclerosis in *Ldlr*–/– mice fed a low-fat atherogenic diet. We fed *Ldlr*–/– mice the Clinton/Cybulsky diet (10% kcal fat, 0.15% cholesterol) and sacrificed mice at 8, 10, or 12 weeks postPCB (2 doses of 1 μmol/kg) or vehicle gavage. To characterize this novel model, we examined the effects of PCB 126 on markers of systemic inflammation, hematological indices, fatty livers, and atherosclerotic lesion size. Mice exposed to PCB 126 exhibited significantly increased plasma inflammatory cytokine levels, increased circulating biomarkers of CVD, altered platelet, and red blood cell counts, increased accumulation of hepatic fatty acids, and accelerated atherosclerotic lesion formation in the aortic root. PCB 126 also increased circulating neutrophils, monocytes, and macrophages as determined by flow cytometry analysis. Exposure to dioxin-like PCB 126 increases inflammation and accelerates atherosclerosis in mice. This low-fat atherogenic diet may provide a useful tool to study the mechanisms linking exposure to lipophilic pollutants to increased risk of CVD.

Key words: dioxin; cardiovascular disease; PCB 126; inflammation; atherosclerosis.

Exposure to lipophilic pollutants has been shown in multiple epidemiological studies to be associated with development of cardiometabolic disease. Population-based studies identified relationships between persistent organic pollutants (POPs), including polychlorinated biphenyls (PCBs), dioxins, and chlorinated pesticides, and multiple clinically relevant risk factors for cardiovascular diseases (CVDs), including increased triglyceride levels, hypertension, and induction of chronic inflammation (Carpenter, 2011; Consonni *et al.*, 2012; Goncharov *et al.*, 2008; Kim *et al.*, 2015; Lind *et al.*, 2012; Uemura, 2012). Dioxin-like pollutants, including the well-studied contaminants PCB 126 and TCDD, are some of the most proinflammatory and toxic man-made POPs known. Although their U.S. manufacturing concluded decades ago, quantifiable levels of both pollutants can still be observed today in the majority of the population (Hopf *et al.*, 2009). In highly exposed cohorts within the United States (eg, Anniston, Alabama), Europe (eg, Seveso, Italy), and Japan (eg, Yusho), dioxin-like pollutants have been linked to increased risk of type-2 diabetes and myocardial infarction (Aminov *et al.*, 2013; Consonni *et al.*, 2012; Goncharov *et al.*, 2010; Kashima *et al.*, 2011; Silverstone *et al.*, 2012).

Dioxin-like pollutants likely modulate CVD and related pathologies by inducing oxidative stress, cellular dysfunction, and chronic inflammation in key cell types associated with atherosclerosis. For example, dioxin-like PCBs have been shown to initiate vascular endothelial cell dysfunction, induce key proatherogenic adhesion molecules, increase monocyte attraction, and induce vascular permeability (Han *et al.*, 2010; Majkova *et al.*, 2009; Petriello *et al.*, 2014). Also, it is well established that atherosclerosis is a chronic inflammatory disease, and dioxin-like pollutants have been shown to induce cytokine production from multiple cell types including adipocytes and endothelial cells (Baker *et al.*, 2013a; Majkova *et al.*, 2009). Furthermore, some evidence now links exposure to dioxin-like chemicals to activation and modulation of immune cells critical to the development and progression of atherosclerosis (Wang *et al.*, 2015).

Animal models are an important approach for understanding the mechanisms linking environmental chemical exposures to disease mechanisms. Robust mouse models of experimentally induced atherosclerosis are well suited for studies of experimental interventions that attenuate development of atherosclerotic lesions (Zadelaar *et al.*, 2007). However, because these models employ genetic and dietary approaches to induce profound hyperlipidemia in mouse strains that are otherwise highly resistant to development of atherosclerosis they are less well suited to studies of agents (eg, toxicants) and mechanisms that might accelerate or otherwise promote development of the disease. A secondary concern is that hyperlipidemia and adipose tissue expansion clearly limit the bioavailability of lipophilic chemicals. For example, it has been shown that mice were protected against deleterious effects of dioxin-like pollutants during a weight gain phase, but exhibited pollutant-induced glucose intolerance and inflammation during a low-fat weight loss phase (Baker *et al.*, 2013b). To address these limitations, we examined the effect of a dioxin like pollutant, PCB126, on the development of atherosclerosis in hypercholesterolemic LDL receptor deficient mice fed a previously described low-fat atherogenic diet. PCB126 robustly accelerated development of atherosclerosis in these animals through mechanisms that involve increased inflammation and pathologies in blood and vascular tissues. This model may be useful for examining the effects of environmental pollutants on experimental atherosclerosis and would enable the use of genetic and pharmacological strategies to investigate relevant mechanisms.

MATERIALS AND METHODS

We fed male *Ldlr–/–* mice a 10% kcal fat, 0.15% cholesterol diet, exposed them to 2 low dose boluses of PCB 126 at the beginning of the study, and examined the pollutant-induced impact on accelerated atherosclerosis and inflammation up to 10 weeks after PCB exposure.

Animals, diet, and study design. The animal protocol was approved by the University of Kentucky Institutional Animal Care and Use Committee. The health of the mice throughout the study was monitored by Division of Laboratory Animal Resources (DLAR) and research staff. The study did not result in undue stress to the mice as determined by behavioral and physiological responses (eg, hunched posture and decreases in food intake). Seven-week-old male *Ldlr–/–* mice were purchased from Jackson Laboratories (Bar Harbor, Maine) and allowed to acclimate for 1 week. Mice were randomly divided into 2 study groups ($n = 30$ per group) with half of the mice receiving 1 μmol/kg PCB 126 (AccuStandard, Connecticut) or safflower oil vehicle (Dyets, Bethlehem, Pennsylvania) at weeks 2 and 4 via gavage. The dose of PCB 126 chosen is more environmentally relevant than past studies from our laboratory which utilized wild-type C57BL/6 mice (Newsome *et al.*, 2014) and produced circulating levels of PCB 126 at the parts per billion range. To promote atherosclerosis in all mice, and to test the hypothesis that dioxin-like PCBs could accelerate atherosclerosis in lean mice, the low-fat proatherogenic Clinton/Cybulsky diet (Teupser *et al.*, 2003) was fed ad libitum (Research Diets, New Brunswick, New Jersey; Product No. D01061401C). The nutrient makeup of the 0.15% cholesterol diet can be found in Supplementary Table 1. Mice were housed in a temperature- and light controlled-room (12 h light:12 h dark) with water ad libitum. Due to the novelty of this proatherogenic model, it was unknown what time-point would be most appropriate to study accelerated atherosclerosis. Thus, mice were sacrificed at 8, 10, or 12 week, postfirst gavage ($n = 10$ per group). Prior to euthanasia, mice were anesthetized and blood was collected via retro-orbital bleed. Ethylenediaminetetraacetic acid (EDTA), and Citrate Theophylline Dipyridamole Adenosine (CTAD) were added to collected blood samples, briefly mixed, and centrifuged at 2000 g for 15 min at 4°C to separate blood plasma. Plasma samples were frozen in liquid nitrogen and stored at −80°C until processing. Prior to the euthanasia of the final set of mice, analysis was performed for lean and body fat composition using EchoMRI (EchoMRI LLC, Houston, Texas).

Quantitation of cytokines and circulating proteins in plasma. The Milliplex Map Mouse Cytokine/Chemokine Magnetic Bead Panel 25-plex (Millipore Corp, Billerica, Massachusetts) was utilized to measure plasma cytokines; while the Milliplex Map Mouse CVD Magnetic Bead Panel 1 was used to measure plasma CVD markers on the Luminex Xmap MAGPIX system (Luminex Corp, Austin, Texas), as per the manufacturer's instructions. Values below the standard curve were denoted as zero for statistical analyses.

Flow cytometry for inflammatory cells. Peripheral blood (PB) samples (50 μl) from the 14-week time point were obtained from the retro-orbital plexus of mice into tubes containing 1:5 ratio of EDTA: CTAD. PB was resuspended in PBS containing 2% fetal bovine serum. Staining was performed for 30 min on ice using monoclonal antibodies against: CD45-APCCy7 (Biolegend, San Diego, CA 103116), CD115-PE (Biolegend, San Diego, CA 135506), CD11b-APC (Biolegend, San Diego, CA 101212), F4/80-PECy7 (Biolegend, San Diego, CA; 123114) and Ly-6 G/Ly6C-PerCPCy5.5 (Biolegend, San Diego, CA 108428). Red blood cells were lysed and cells were fixed

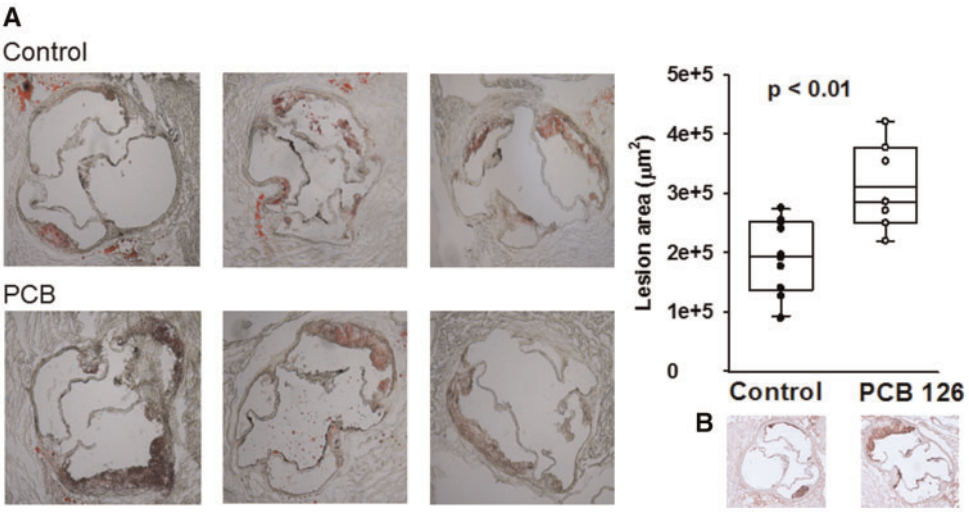

Figure 1. PCB 126 accelerates atherosclerosis at 12 weeks in mice fed a high cholesterol diet. Male *Ldlr*–/– mice were fed a low fat, 0.15% cholesterol diet and administered 1 μmol/kg PCB 126 at weeks 2 and 4. Aortic roots were frozen and serially sectioned from the emergence of the 3 valves. On average, the mean of 6 sections per mouse was utilized for quantitation. A, Shown are Oil Red O stained aortic root sections of mice exposed to vehicle control or PCB 126 with associated lesion area quantification ($n = 10$ control, $n = 7$ PCB; $p < .01$; Student's *t*-test). B, Shown is CD68 staining by IHC which illustrates the early nature of the lesions with evident macrophage infiltration. The box and whisker plots show individual data points and also the median, mean, and error bars for each group.

using 1x lyse/fix buffer (BD Pharmingen, San Jose, CA 558049). Monocyte subsets (CD45+/CD115+/Ly6Chi and Ly6Clo), inflammatory macrophages (CD45+/F4/80+/CD11b+) and neutrophils (CD45+/CD115-/Ly-6 G+/C+) were analyzed using LSR II (Becton Dickinson, Mountainview, California). Flow cytometry data was analyzed using Flow Jo software version 7.6 (Tree Star, Ashland, Oregon). Similarly, splenic populations were determined by staining the cell suspension with CD11b (PerCP-cy5.5, clone M1/70, BD Phamingen), Gr-1 (FITC, Biolegend, San Diego, CA, clone RB6-8C5), F4/80 (PE, Thermo Fisher, clone BM8) at 1:200 dilution for 30 min on ice. Samples were washed twice with FACS buffer, suspended in FACS buffer, and analyzed on the LSR II.

Hematological analyses. To examine hematological changes at the earliest time point, the Hemavet 950 FS instrumentation (Drew Scientific Group, Miami Lakes, FL) was utilized per the manufacturer's instructions.

Quantitation of atherosclerotic lesions. To quantify extent of atherosclerosis, aortic roots were frozen in O.C.T. Compound (Fisher Scientific, Pittsburgh, PA), sectioned at 10 μm per section, and stained with oil red O as described before in Paigen *et al.* (1987). Briefly, serial sections were collected as close as possible to the observed emergence of the 3 valves, and sections were placed on microscope slides (Probe-on Plus; Fisher Scientific, Pittsburgh, Pennsylvania) until the aortic valves disappeared. Frozen sections were lipid stained with oil red O, and images were taken using a Nikon Eclipse (Melville, NY) 55iUpright microscope attached to a 12 MP color camera. Subsequent images were quantified for lesion area by Image-Pro Software Plus 4.5. For the results shown in Figure 1, the average of approximately 6 serial sections per mouse were used for quantification. In addition, *En Face* analysis of the aortic arch was undertaken. Whole aortas were cleaned of adventitial tissue, excised from the heart, and placed in 10% formalin for 24 h. The aorta was opened by cutting through the innominate artery, left common carotid artery, left subclavian artery, and inner curvature. Aortic arches were pinned flat on black wax, imaged, and percent lesion area was determined with Image-Pro Software Plus 4.5.

Lipid profiles. Plasma total cholesterol (Infinity Cholesterol, ThermoScientific, USA), triglyceride (TRIGS, Randox, UK), phospholipid (Phospholipids C, Wako Pure Chemical Industries, Japan), and free fatty acid (Reagent A/B, Wako, Pure Chemical Industries, Japan) concentrations were determined via colorimetric kits, as per the manufacturer's instructions.

RNA isolation and polymerase chain reaction amplification. Liver samples were homogenized and mRNA was isolated with TRIzol reagent (Invitrogen, Carlsbad, California) according to the manufacturer's protocol. mRNA concentrations was then determined using a NanoDrop 2000 spectrophotometer (Thermo Scientific, Waltham, Massachusetts). Reverse transcription was performed using the AMV reverse transcription system (Promega, Madison, Michigan). mRNA levels of multiple lipid regulated genes were determined by quantitative real-time polymerase chain reaction (PCR) using an Applied Biosystems QuantStudio 7 Flex Real-Time PCR system (Thermo Scientific, Waltham, Massachusetts) and Taqman fast reagents (Applied Biosystems). The MS Lipid regulated genes plate (No. 4418846, ThermoScientific) contained dried taqman primers, and HPRT1 was used as the housekeeping control for ΔΔCt relative quantitation.

Hepatic fatty acid analyses. Hepatic fatty acids/lipids were extracted and analyzed by Metabolon (Durham, North Carolina). Samples were prepared using the automated MicroLab STAR system from Hamilton Company. Several recovery standards were added prior to the first step in the extraction process for QC purposes. To remove protein, small molecules bound to protein were dissociated or trapped in the precipitated protein matrix, and to recover chemically diverse metabolites, proteins were precipitated with methanol under vigorous shaking for 2 min (Glen Mills GenoGrinder 2000) followed by centrifugation. Lipids were extracted in the presence of authentic internal standards using chloroform: methanol (2:1 v/v). For the separation of neutral lipid classes (eg, FFA) a solvent system consisting of petroleum ether/diethyl ether/acetic acid (80:20:1) was employed. Each lipid class was transesterified in 1% sulfuric acid in methanol in a sealed vial under a nitrogen atmosphere

at 100 °C for 45 min. The resulting fatty acid methyl esters were extracted from the mixture with hexane containing 0.05% butylated hydroxytoluene and prepared for GC by sealing the hexane extracts under nitrogen. Fatty acid methyl esters were separated and quantified by capillary GC (Agilent Technologies 6890 Series GC) equipped with a 30 m DB 88 capillary column (Agilent Technologies, Santa Clara, CA) and a flame ionization detector.

PCB 126 quantitation. PCBs from livers and plasma were extracted and cleaned using a modified dispersive solid phase extraction method (Smith and Lynam, 2012). In total 20–30 mg of liver tissue samples/50 μl plasma was weighed out into a centrifuge tube. 50 μl of 5 μM internal standard (13C12-PCB 126; Cambridge Isotopes, Tewksbury, Massachusetts), 400 μl deionized water and 400 μl acetonitrile containing 1% acetic acid were added to each tube. The tissue samples were homogenized using stainless steel beads and a Next Advance Bullet Blender (Troy, New York). The samples were vortexed for 1 min followed by centrifugation at 4000 rpm for 5 min. The upper layer was transferred to an Agilent (Agilent Technologies, Santa Clara, CA) Bond Elut QuEChERS fatty sample dispersive 2 ml SPE column, vortexed for 1 min and centrifuged at 13 000 rpm for 4 min. The supernatant was transferred to a 4 ml vial and dried under nitrogen. The sample was reconstituted in 100 μl isooctane and transferred to a GC vial. PCB 126 was analyzed using an Agilent (Agilent Technologies, Santa Clara, CA) GC-triple quadrupole MS (GC-MS/MS) 7000 C system equipped with a multimode inlet and a HP-5MS UI column (30 m, 0.25 mm, and 0.25 μm) in multiple reaction monitoring mode. Ion transitions monitored were 325.9/255.9 for PCB 126 and 337.9/267.9 for 13C12-PCB 126 internal standard. Relative quantitation was done by comparing peak area of the sample to peak area of an internal standard sample of known concentration.

Statistical analyses. Data were analyzed using SigmaStat software (Systat Software, Point Richmond, California). Comparisons between treatments were determined by Student's *t*-test or Mann-Whitney rank sum test depending on normality and variance distributions. Sample sizes for each experiment are indicated in corresponding figure legends (eg, qRT-PCR mRNA analysis $n = 5$, aortic root lesion quantitation $n = 7$–10). A probability value of $p < .05$ was considered statistically significant. For hepatic fatty acid analyses, a Welch's 2-sample *t*-test was used to determine differences between vehicle control and PCB 126-treated mice ($n = 6$ per group). These analyses were performed using ArrayStudio (Qiagen) on log transformed data.

RESULTS

PCB 126 Accelerates Atherosclerosis in Lean Ldlr–/– *Mice*

We quantified Oil Red O-staining within aortic roots of *Ldlr–/–* mice fed a low-fat atherogenic diet for 12 weeks (10 weeks postfirst PCB gavage) and determined that PCB-exposed mice displayed significant increases in lesion area compared with vehicle controls (Mean control; $2.04 \times 10^5 \pm 1.68 \times 10^4$ μm^2, Mean PCB; $3.11 \times 10^5 \pm 2.78 \times 10^4$ μm^2, $p < .01$; Figure 1). These sections were also immunohistochemical (IHC) stained for CD68 and it was determined that the lesions were representative of early, macrophage-laden atheromas (Figure 1B). To confirm the accelerated atherosclerosis findings, aortic roots from the 10 week time point (8 weeks postfirst PCB gavage) were also serially sectioned and stained for lipids. As expected at 10 weeks, quantified lesions had less surface area compared with the 12-week samples, but again, PCB-exposed mice exhibited accelerated atherosclerosis (Mean control; $9.56 \times 10^4 \pm 1.19 \times 10^4$ μm^2, mean PCB; $2.12 \times 10^5 \pm 4.53 \times 10^4$ μm^2, $p < 0.05$). We then investigated lesion formation within the aortic arch via *en face* method in mice fed diet for 12 weeks. Differences in lesion area between PCB and vehicle control mice were not as apparent as in the aortic root, and no significant difference was observed (mean control; 9.14% ± 1.23% lesion/arch area, mean PCB; 11.94% ± 1.79% lesion/arch area, $p = .2$; data shown in Supplementary Materials). To characterize this novel model of pollutant-accelerated atherosclerosis, we next examined effects on cytokine production, circulating inflammatory mediators, and hepatic lipid accumulation.

Dioxin-like PCB 126 Increases Circulating Levels of Proinflammatory Proteins and CVD-Biomarkers

Since cytokine release is a critical marker of early stage inflammation and atherosclerosis, we determined concentrations of a panel of these proteins in plasma harvested examined plasma concentrations of a panel of these proteins from mice fed the low-fat atherogenic diet for 10 weeks. Using the Magpix multiplex technology we determined that PCB 126 significantly increased granulocyte-colony stimulating factor (G-CSF), Interferon gamma (IFNγ), interleukin 1 beta (IL-1β), IL-12 (p70), and IL-13 compared with vehicle control (Figure 2). In addition, IL-10, IFNγ-induced protein 10 (IP-10), and tumor necrosis factor (TNFα) also trended toward being significantly increased ($p = .10$) (Figure 2). As atherosclerosis progressed (eg, 14 wks on diet), differences in circulating cytokines between PCB 126 and vehicle control mice diminished (data not shown). In addition, we examined circulating levels of CVD-related biomarkers by combining data from all 3 time-points and determined that PCB 126 administration increased sICAM-1 and PAI-1, but decreased sP-Selectin ($p < .05$; $n = 30$ per group; data shown in Supplementary Materials). Also, plasma concentrations of proMMP-9 were below the standard curve in all mice, but mean fluorescent intensity as determined by suspension array methods was significantly increased in PCB administered mice ($p < .01$; $n = 30$ per group).

PCB 126 Modulates Hematological Parameters Consistent with Anemia of Inflammation

A growing body of evidence implicates exposure to dioxin-like pollutants and induction of chronic inflammation. One consequence of inflammation that can relate to atherosclerosis is anemia and subsequent thrombocytosis (elevated platelets). Therefore, we examined hematological parameters of mice fed the low-fat atherogenic diet for 10 weeks using the Hemavet veterinary system (Figure 3). PCB 126 significantly increased number of circulating platelets (approximately 20%) and decreased hematocrit, hemoglobin, and red blood cell levels ($p < .05$). Also, PCB 126 decreased the size distribution spread of the erythrocyte population as well as the monocyte percentage, and increased the overall percentage of lymphocytes within the sample ($p < .05$).

PCB 126 Increases Abundance of Atherosclerosis-Related Leukocyte Populations in PB and Spleen

Since it was determined via Hemavet analysis that PCB 126 exposure impacts hematological parameters at the early 10 week time-point, we next investigated if effects on monocytes, macrophages, and neutrophils were apparent in mice fed diet for 14 weeks. Using flow-cytometry and antibodies specific to monocyte sub populations (Figure 4), we determined that mice exposed to PCB 126 exhibited higher levels of circulating Ly6 low

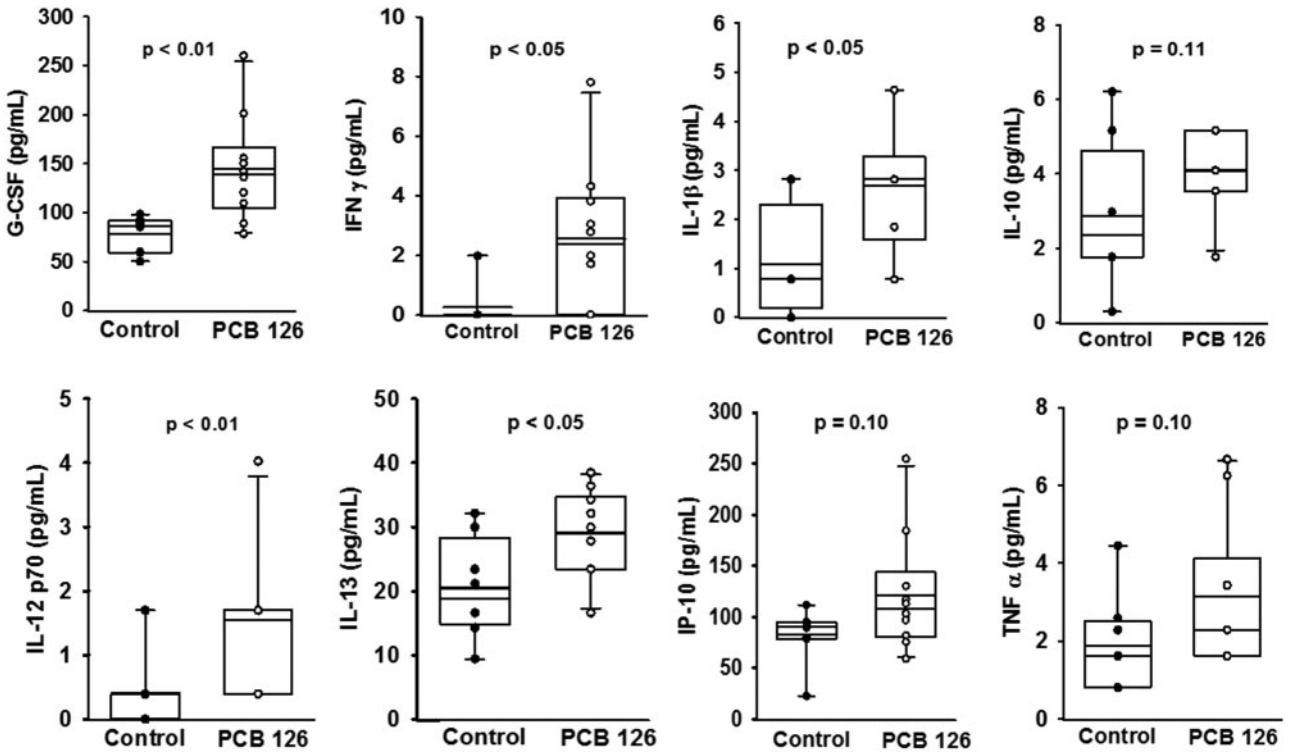

Figure 2. Analysis of circulating cytokines showed that PCB 126 increases systemic inflammation at 10 weeks in mice fed a high-cholesterol diet. Male *Ldlr–/–* mice were fed a low fat, 0.15% cholesterol diet and exposed to 1 μmol/kg PCB 126 at weeks 2 and 4. PCB exposure increased plasma levels of G-CSF, IFNγ, IL-1β, IL-12 (p70), and IL-13 compared with vehicle safflower oil control (magpix technology; $p < .05$). IL-10, IFNγ-IP-10, and TNFα were not significantly increased in PCB administered mice ($p = .10$). The box and whisker plots show individual data points and also the median, mean, and error bars for each group. Statistical significance was determined by Student's *t*-test or Mann-Whitney rank sum test depending on normality and variance distributions.

($p = .01$) and Ly6 high ($p = .13$) monocytes. We also identified an approximately 3-fold increase in F4/80 positive, CD11b positive macrophages circulating in PB ($p < .01$). Interestingly, we also observed a 3-fold increase in circulating neutrophils in mice exposed to PCB 126 and fed the low-fat atherogenic diet for 14 weeks ($p < .01$). To confirm these results we also examined F4/80 positive, CD11b positive macrophages in spleen tissue of these same mice and saw a significant increase in PCB 126-treated mice ($p < .05$; data shown in the Supplementary Materials). Also in the spleen, CD11b positive, GR-1 positive cell types were significantly more abundant in PCB 126 exposed mice ($p < .01$).

PCB 126 Increases Hepatic Lipid Accumulation and Modulates the Expression of Lipid-Regulated Genes

Hepatic lipid accumulation and steatosis are risk factors for atherosclerosis, thus the progression of PCB-induced liver disease was examined in *Ldlr–/–* mice fed a low-fat atherogenic diet (Lonardo *et al.*, 2013). As determined by a liver pathologist, pollutant exposure increased lipid droplet formation within hepatocytes leading to significant micro-vesicular fatty change in centrilobular areas in mice fed diet for both 10 and 14 weeks. These changes were not observed in vehicle control animals. At these time points no fibrosis or steatohepatitis was observed in any groups. Using GC-MS/MS, we quantitated PCB 126 in livers and plasma from mice fed diet for 10 weeks and determined that PCB 126 levels were approximately 100 times higher in livers compared with plasma (Mean liver; 2976.0 picograms/mg liver ± 536.2, Mean plasma; 33.9 picograms/μl plasma ± 18.1, $p < .01$; data shown in Supplementary Material). Using qPCR, we then investigated the hepatic expression of a panel of genes regulated by lipids. We identified significant increases in multiple genes due to PCB-exposure including fatty acid translocase (CD36), IL-1β, lipoprotein lipase (LPL), and insulin induced gene 1 (INSIG-1), as well as significant decreases in genes including fatty acid desaturase 1 (Fads1), stearoyl-CoA desaturase 1 (Scd1), and glycerokinase (Gyk) (Figure 5). Finally, we utilized targeted GC MS to quantitate fatty acid abundances in livers of these mice. Exposure to PCB 126 resulted in broad increases in nearly all long chain, polyunsaturated, and branched chain fatty acids examined (Table 1; red-shading denotes induction at $p < .05$).

PCB 126 Alters Body Composition and Plasma Lipid Profiles in Lean Mice Fed the Atherogenic Diet

Studies utilizing *Ldlr–/–* mice commonly use a high fat/high cholesterol Western style diet that can lead to obesity and extreme atherogenic phenotypes. In this study a low-fat atherogenic diet led to slow consistent weight gain (approximately 22 g at start to approximately 30 g at week 14; data shown in Supplementary Materials) and no wasting syndrome following PCB dosing (ie, no loss of body weight following PCB gavage). There were no differences in body weight or food intake between vehicle control mice and PCB-exposed mice. Interestingly, at 14 weeks, PCB-treated mice exhibited decreased percent lean mass and increased percent fat mass compared with controls (echoMRI; data shown in Supplementary Materials). The liver-to-body weight ratio was also significantly increased in PCB-treated mice at this time (Mean control; $3.73 \times 10^{-2} \pm 7.52 \times 10^{-4}$, mean PCB; $4.63 \times 10^{-2} \pm 1.59 \times 10^{-3}$, $p < .01$). Finally, to investigate if the observed PCB-accelerated atherosclerosis could be attributed to simply increases in circulating cholesterol or triglycerides, we completed lipid profiles for mice at all 3 time points

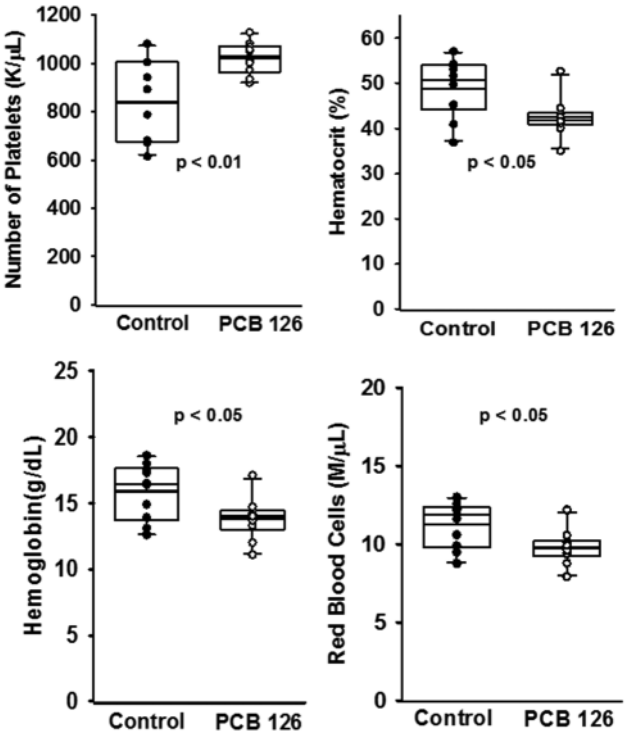

Figure 3. Analysis of circulating hematological parameters showed that PCB 126 may lead to anemia of inflammation at 10 weeks in mice fed a high cholesterol diet. Male *Ldlr–/–* mice were fed a low fat, 0.15% cholesterol diet and exposed to 1 μmol/kg PCB 126 at weeks 2 and 4. Whole blood was collected at sacrifice and analyzed for blood cell parameters via hemavet instrumentation. PCB 126 exposure increased circulating platelet counts and decreased circulating red blood cell counts in conjunction with a decreased hematocrit and hemoglobin concentration ($n = 10$ per group; $p < .05$). The box and whisker plots show individual data points and also the median, mean, and error bars for each group. Statistical significance was determined by Student's *t*-test or Mann-Whitney rank sum test depending on normality and variance distributions.

(data shown in Supplementary Materials). Interestingly, total plasma cholesterol levels were decreased in PCB-treated mice at all 3 time points (but still close to 500 mg/dl) and triglyceride levels were only different at 14 weeks.

DISCUSSION

Since hyperlipidemia and adipose tissue expansion may limit the bioavailability of lipophilic chemicals, we examined the effect of a dioxin like pollutant, PCB126, on the development of atherosclerosis in hypercholesterolemic LDL receptor-deficient mice fed a previously described low-fat atherogenic diet. PCB126 robustly accelerated development of atherosclerosis in these animals through mechanisms that likely involve increased systemic inflammation and effects on blood and vascular cells. Here, we have validated a low-fat diet capable of quickly promoting lesion formation in *Ldlr–/–* mice without the added stress and variable of large weight gain. Also, data described here clearly show that PCB 126 can contribute independently to inflammation and atherosclerosis in the *Ldlr–/–* mouse model. It will be important to follow-up these observations using additional lipophilic toxicants to determine the broader use of this model. Also, future studies should use additional techniques to quantify atherosclerotic progression including arterial imaging or Doppler ultrasound.

Inflammation of multiple cell types is a critical early mediator of atherosclerosis. It is well established in cell culture models that exposure to dioxin-like pollutants can elicit endothelial cell, adipocyte, and macrophage inflammation (Sciullo *et al.*, 2010). Aryl hydrocarbon receptor (AhR) activation coupled to alterations of redox signaling appear to be critical mediators of these deleterious effects. Here, we show that at the earliest time point examined, (eg, 10 weeks on diet) PCB 126-exposed mice exhibited significantly higher circulating cytokines and proinflammatory mediators (Figure 2). PCB 126 significantly increased G-CSF, IFNγ, IL-1β, IL-12 (p70), and IL-13 compared with vehicle control, but IL-10, IP-10, and TNFα were not significantly changed ($p = .1$). IL-10 is an anti-inflammatory cytokine that is involved with the resolution of inflammation, but it is unclear why TNFα and IP-10 did not follow the same pattern as the other increased proinflammatory mediators (Couper *et al.*, 2008). Importantly, we observed accelerated lesion formation at both weeks 10 and 12 (week 14 not examined), and it is predicted that future studies examining even earlier time points may be beneficial. Clinically, identifying biomarkers that can predict adverse cardiovascular events or that are associated with atherosclerosis are a critical area of study. Known biomarkers include circulating cytokines and adhesion molecules (eg IL-1β and ICAM-1), lipoproteins/triglycerides, and emerging markers such as trimethylamine-N-oxide (Bennett *et al.*, 2013). In a population-based study, circulating levels of ICAM-1 and VCAM-1 were positively associated with multiple dioxin-like pollutants including PCB 126 (Kumar *et al.*, 2014). Here we provide evidence that PCB 126 can increase circulating sICAM-1, PAI-1, and proMMP-9 in *Ldlr–/–* mice fed the low-fat atherogenic diet. Importantly, some of these biomarkers may have causal roles in coronary heart disease progression and severity. For example, PAI-1, which has also been shown to be increased in other PCB 126 studies, has been shown to associate with heart disease incidence, independent of other risk factors. Emerging data now implicate PAI-1's role not only in clot formation/stability, but also in circulating fasting glucose levels (Song *et al.*, 2017).

Two other nontraditional risk factors for CVD, anemia and fatty livers, have been associated with dioxin-like pollutant exposure (Geusau *et al.*, 2001; Guo *et al.*, 1999; Lonardo *et al.*, 2013; Serdar *et al.*, 2014). Chronic anemia and anemia of inflammation have been linked to multiple cardiovascular pathologies including cardiac enlargement, left ventricular hypertrophy, and tissue hypoxia (Mozos, 2015). In the current study, we observed a significant decrease in hematocrit and hemoglobin levels; 2 markers used clinically to identify anemic states. The observed anemia may have been caused by the increased inflammation, a decrease in red blood cell formation, or alteration of iron homeostasis. As in our study, a positive association between PCB exposure and neutrophil and platelet counts was observed in a recent population-based study of Chinese e-waste recyclers; however a positive association with hemoglobin levels was observed (Xu *et al.*, 2015). Also, it is well established that dioxin-like pollutant activation of AhR, and subsequent upregulation of cytochrome P450s (eg, Cyp1a1) can lead to the complexation of iron by pollutants and decreased cellular iron availability (Schreinemachers and Ghio, 2016). Although the anemic phenotype likely did not play a major role in our observed accelerated atherosclerosis, future longer term studies may be useful to identify a link between dioxin-like pollutant exposure, anemia, and more progressive CVD pathologies (eg, left ventricular hypertrophy). Dysregulated hepatic fat accumulation and specifically nonalcoholic fatty liver disease (NAFLD) are linked to diabetes, kidney disease, and CVD (Lonardo *et al.*, 2013). Patients

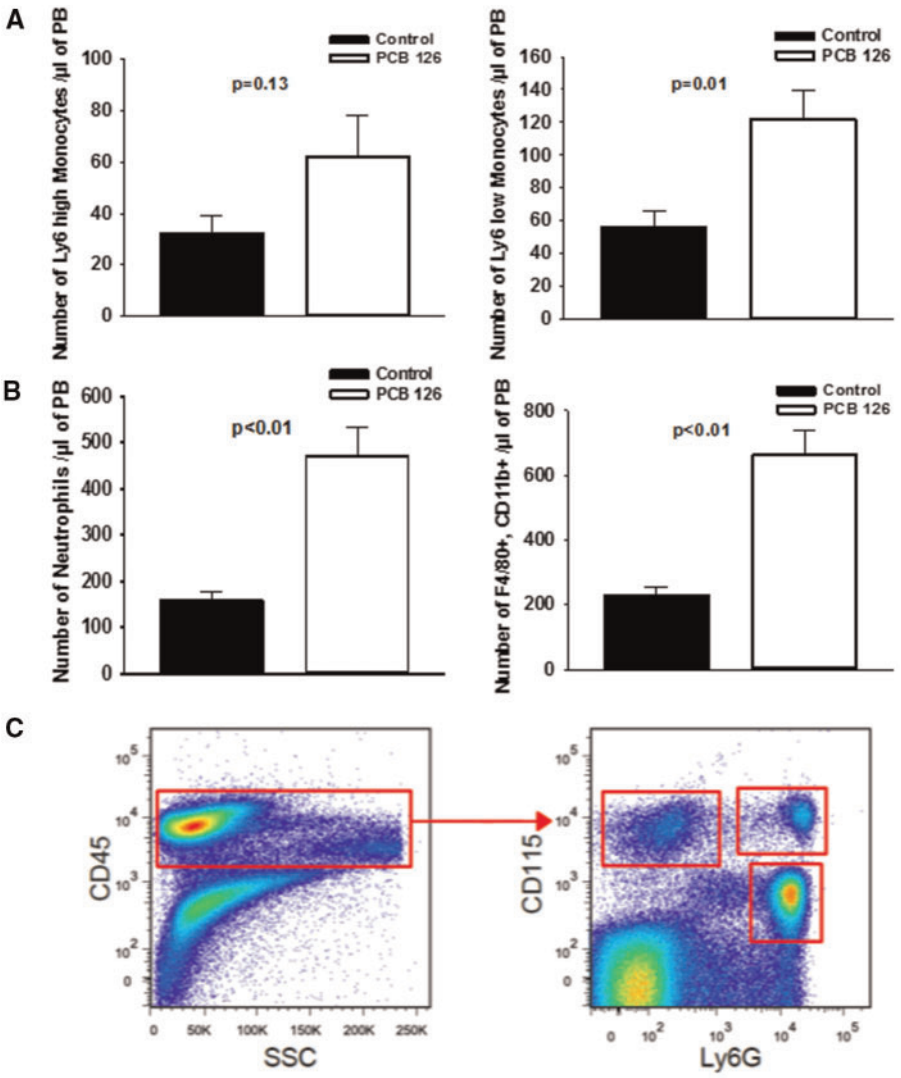

Figure 4. Dioxin-like PCB 126 is associated with increased PB inflammatory cells. Exposure to PCB 126 increases circulating levels of monocytes, macrophages, and neutrophils at 14 weeks in mice fed a high-cholesterol diet. PB was collected at sacrifice and blood cell types were isolated by flow cytometry. Quantitative analyses of monocyte subpopulations in PB demonstrating an increase in PB monocyte subpopulations (Panel A). Similarly, significant increase in neutrophils and inflammatory macrophages was observed in PB samples (Panel B). Representative FACS plots demonstrating the gating strategy for Ly6Chi (CD45+/CD115+/Ly6C-G+), Ly6Clo (CD45+/CD115+/Ly6C-G−) monocytes and neutrophils (CD45+/CD115−/Ly-6 G+/C+) (Panel C). Data are presented as mean ± SEM ($n = 5$ per group). Statistical significance was determined by Student's t-test or Mann-Whitney rank sum test depending on normality and variance distributions.

with NAFLD were shown to have elevated C-reactive protein, increased mean carotid intima-media thickness, and higher plaque prevalence than matched controls (Brea *et al.*, 2005). More work need to be done to elucidate a causative link between a compromised liver and atherosclerosis risk. In our study, significant microvesicular fatty change in centrilobular areas was observed in mice exposed to PCB 126. Clinically, NAFLD liver biopsies usually show macrovesicular steatosis but do sometimes present as microvesicular (Tandra *et al.*, 2011). Diffuse microvesicular steatosis is usually related to etiologies related to toxin exposure. Also, PCBs induced the expression of multiple lipid regulated genes including CD36, which has important fatty acid uptake functions (Xu *et al.*, 2013). Also, we observed a decrease in Fads1 expression which the enzyme's activity has recently been linked to NASH and considered a bottleneck leading to fatty acid accumulation (Chiappini *et al.*, 2017). The administered PCB dose resulted in hepatomegaly which has been observed in previous studies (Klaren *et al.*, 2016, Wahlang *et al.*, 2017). Ultimately, we observed broad increases in hepatic fatty acid species in PCB-exposed mice, but future longer term studies are necessary to determine if this model will be useful to study the effects of NAFLD, steatohepatitis, and cirrhosis in lean individuals.

It is well established that dioxin-like lipophilic pollutants, such as PCBs, sequester within adipose stores and that obese individuals have higher total body burdens of POPs. However, some epidemiological studies have observed an inverse relationship with BMI and relative risk of pollutant-associated diseases. For example, using NHANES data from 1994 to 2004, researchers determined that significant interactions between fat mass and POPS were evident, and that in elderly patients with higher POP concentrations a negative association with mortality was determined (Hong *et al.*, 2012). Using the same dataset, another group showed that, in elderly individuals with low-fat mass, PCBs were positively associated with an increased risk of CVD mortality, but this association was eliminated in

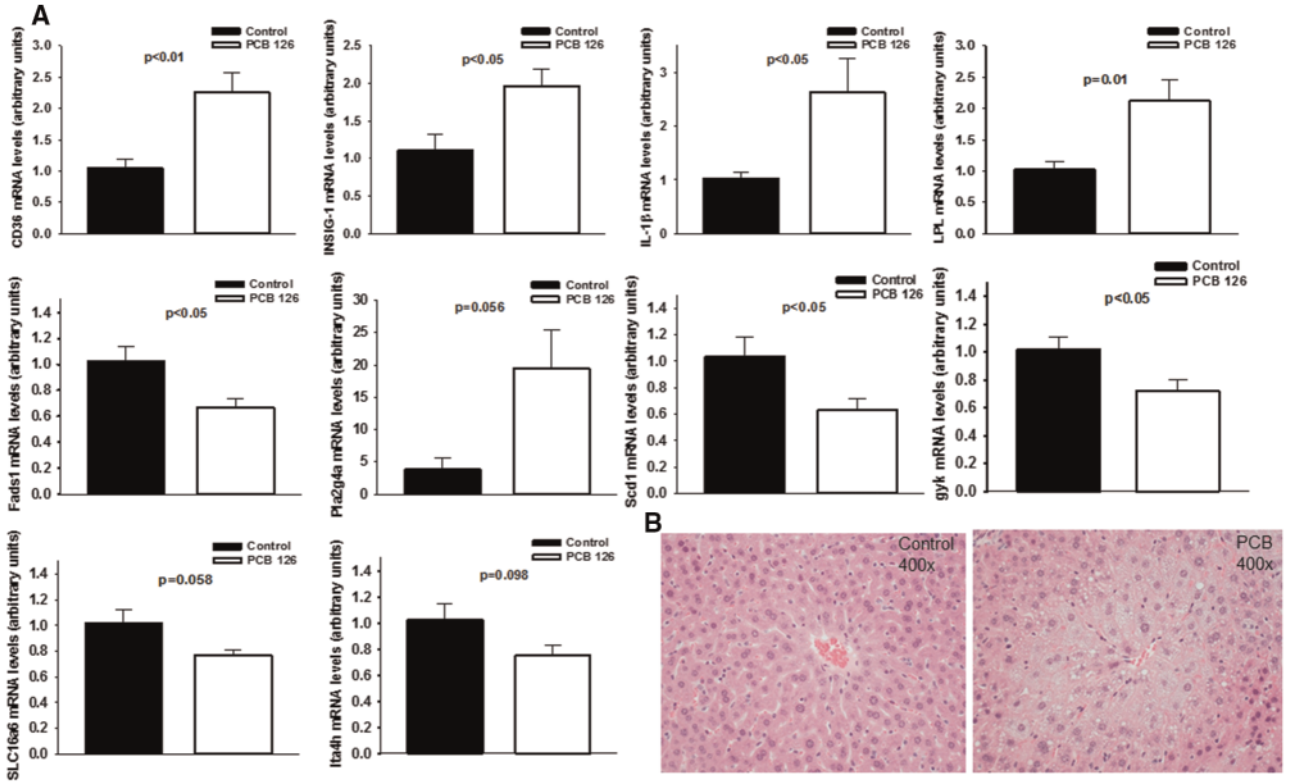

Figure 5. Exposure to PCB 126 modulates hepatic lipid accumulation at 14 weeks in mice fed a high cholesterol diet. Male *Ldlr–/–* mice were fed a low fat, 0.15% cholesterol diet and exposed to 1 μmol/kg PCB 126 at weeks 2 and 4. All mRNA values were determined using the relative quantification method (ΔΔCt) and normalized to control. Hprt1 was used as the housekeeping gene for all mRNA quantifications. A, PCB 126 increased hepatic mRNA levels of fatty acid translocase (CD36), INSIG-1, IL-1β, LPL, Phospholipase A2 Group IVA, and downregulated Fads1, Scd1, Gyk, Solute Carrier Family 16 Member 6, and leukotriene A4 hydrolase. Data are presented as mean ± SEM ($n = 5$ per group; Student's *t*-test). B, Shown are representative H&E stained hepatic sections which illustrate the observed PCB-induced significant microvesicular fatty change in centrilobular regions.

individuals with higher fat mass (Kim *et al.*, 2015). Also, multiple animal studies support the hypothesis that increased adiposity and subsequent sequestration can protect other organ systems from the deleterious effects of environmental pollutants (Baker *et al.*, 2013b; La Merrill *et al.*, 2013; Tuomisto *et al.*, 1999). Early toxicological work showed that animals with higher fat mass required larger concentrations of toxicant to produce a negative outcome (Geyer *et al.*, 1993; Lassiter and Hallam, 1990). Lipophilic pollutants have been shown to exert negative effects during weight loss, but not during a high fat fed weight gain phase. For example, it has been shown that mice were protected against deleterious effects of dioxin-like pollutants during a weight gain phase, but exhibited pollutant-induced glucose intolerance and inflammation during a low-fat weight loss phase (Baker *et al.*, 2013b). Importantly, it is known that PCBs can covalently bind to lipid species which may alter enterohepatic circulation and/or excretion (Morck *et al.*, 2002). More work need to be done to determine if any of the observed inverse associations with BMI and pollutant-induced disease can be attributed to these observations. Here, we have proposed and validated a model of accelerated atherosclerosis using the *Ldlr–/–* mouse that can bypass these concerns.

Although this appears to be the first example of dioxin-like pollutant-acceleration of atherosclerosis in the *Ldlr–/–* model, other groups have previously demonstrated similar effects using the ApoE deficient mouse. Observing proatherogenic effects in both models is important, because the etiology and ability to mirror the human condition do differ in the ApoE and *Ldlr* models (Getz and Reardon, 2016). In one study examining chronic intraperitoneal injection of TCDD, researchers observed increased foam cell formation and lesion size in the aorta (Wu *et al.*, 2011). Another group showed that injection of dioxin-like PCB 77 modulated cholesterol levels, adipocyte inflammation, and lesion formation (Arsenescu *et al.*, 2008). Finally, to study the impact of mixtures of dioxin-like pollutants on atherogenesis, another group injected male ApoE–/– mice with a complex mixture of PCBs (Aroclor 1254) and TCDD separately or in combination and saw increased lesion formation in both the TCDD alone and TCDD + Aroclor groups (Shan *et al.*, 2014). The *Ldlr–/–* model has previously been used to examine PCB-induced inflammation in hepatic and aortic tissues. For example, it was shown that injection of PCB 77 could increase hepatic lipid accumulation and aortic VCAM-1 staining and this was dependent on the fat makeup of the diet (Hennig *et al.*, 2005). This work was later expanded via microarray analysis and it was determined that the dietary fat content of diets played an important role in what genes exhibited PCB-induced dysregulation (eg, significant interaction between fat content and PCB treatment) (Arzuaga *et al.*, 2009). The work described herein adds to the growing body of evidence that dioxin-like pollutants can independently induce chronic inflammatory responses and modulate risk related to atherosclerosis and CVD. This model may be useful for examining the effects of environmental pollutants on experimental atherosclerosis and would enable the use of genetic and pharmacological strategies to investigate relevant mechanisms.

Table 1. Hepatic Fatty Acid Profiles

Subpathway	Biochemical Name	Fold of Change PCB126 vs. VEH
Medium chain fatty acid	Caproate (6: 0)	1.967
	5-Dodecenoate (12: 1n7)	1.1949
Long chain fatty acid	Myristate (14: 0)	**1.6483**
	Myristoleate (14: 1n5)	**1.5047**
	Pentadecanoate (15: 0)	**1.3333**
	Palmitate (16: 0)	**1.4202**
	Palmitoleate (16: 1n7)	**1.689**
	Margarate (17: 0)	**1.8135**
	10-Heptadecenoate (17: 1n7)	**2.1296**
	Stearate (18: 0)	**1.3224**
	Oleate/vaccenate (18: 1)	**1.8901**
	Nonadecanoate (19: 0)	**1.7897**
	10-Nonadecenoate (19: 1n9)	**2.4285**
	Arachidate (20: 0)	**2.1044**
	Eicosenoate (20: 1)	**3.4008**
	Behenate (22: 0)*	1.4465
	Erucate (22: 1n9)	**2.8541**
	Nervonate (24: 1n9)*	1.3063
Polyunsaturated fatty acid (n3 and n6)	Heneicosapentaenoate (21: 5n3)	**3.933**
	Hexadecadienoate (16: 2n6)	**2.2067**
	Stearidonate (18: 4n3)	**1.5706**
	Eicosapentaenoate (EPA; 20: 5n3)	1.2174
	Docosapentaenoate (n3 DPA; 22: 5n3)	**1.985**
	Docosahexaenoate (DHA; 22: 6n3)	1.2193
	Docosatrienoate (22: 3n3)	**2.5254**
	Nisinate (24: 6n3)	1.211
	Linoleate (18: 2n6)	**1.835**
	Linolenate [alpha or gamma; (18: 3n3 or 6)]	**1.8176**
	Dihomo-linolenate (20: 3n3 or n6)	**2.5076**
	Arachidonate (20: 4n6)	1.1887
	Adrenate (22: 4n6)	1.3929
	Docosapentaenoate (n6 DPA; 22: 5n6)	1.3923
	Docosadienoate (22: 2n6)	**2.6117**
	Dihomo-linoleate (20: 2n6)	**3.0053**
	Mead acid (20: 3n9)	1.2317
	Docosatrienoate (22: 3n6)*	**1.8835**
Fatty acid, branched	15-Methylpalmitate (i17: 0)	**1.5624**
	17-Methylstearate (i19: 0)	**1.7984**

Hepatic fatty acid methyl esters were quantitated and significant differences were determined by Welch's two-sample *t*-tests. Red shading and bold values denotes significantly increased lipid abundance in PCB 126-treated mice (fold change compared to Vehicle; $p < .05$).

SUPPLEMENTARY DATA

Supplementary data are available at *Toxicological Sciences* online.

FUNDING

This work was supported by the National Institute of Environmental Health Sciences at the National Institutes of Health (P42ES007380). Dr A.A.-L. is supported by the University of Kentucky Clinical and Translational Science Pilot Award (UL1TR000117) and the UK COBRE Early Career Program (P20 GM103527). Research reported in this publication was supported by an Institutional Development Award (IDeA) from the National Institute of General Medical Sciences of the National Institutes of Health under (P20GM103527). The UK Flow Cytometry & Cell Sorting core facility is supported in part by the Office of the Vice President for Research, the Markey Cancer Center and an NCI Center Core Support Grant (P30 CA1775) to the University of Kentucky Markey Cancer Center. Lipid profiles were completed by the University of Cincinnati Medical Center MMPC (U24 DK059630). The content is solely the responsibility of the authors and does not necessarily represent the official views of the National Institutes of Health.

ACKNOWLEDGMENTS

All authors were involved in the formulation, design, data acquisition, or data analysis of this study, in addition to drafting and revising the article. All authors acknowledge that the analyses were completed ethically and to the best of their abilities.

REFERENCES

Aminov, Z., Haase, R. F., Pavuk, M., and Carpenter, D. O. (2013). Analysis of the effects of exposure to polychlorinated biphenyls and chlorinated pesticides on serum lipid levels in residents of Anniston, Alabama. *Environ. Health* **12**, 108.

Arsenescu, V., Arsenescu, R. I., King, V., Swanson, H., and Cassis, L. A. (2008). Polychlorinated biphenyl-77 induces adipocyte differentiation and proinflammatory adipokines and promotes obesity and atherosclerosis. *Environ. Health Perspect.* **116**, 761–768.

Arzuaga, X., Ren, N., Stromberg, A., Black, E. P., Arsenescu, V., Cassis, L. A., Majkova, Z., Toborek, M., and Hennig, B. (2009). Induction of gene pattern changes associated with dysfunctional lipid metabolism induced by dietary fat and exposure to a persistent organic pollutant. *Toxicol. Lett.* **189**, 96–101.

Baker, N. A., English, V., Sunkara, M., Morris, A. J., Pearson, K. J., and Cassis, L. A. (2013a). Resveratrol protects against polychlorinated biphenyl-mediated impairment of glucose homeostasis in adipocytes. *The Journal of Nutritional Biochemistry* **24**, 2168–2174.

Baker, N. A., Karounos, M., English, V., Fang, J., Wei, Y., Stromberg, A., Sunkara, M., Morris, A. J., Swanson, H. I., and Cassis, L. A. (2013b). Coplanar polychlorinated biphenyls impair glucose homeostasis in lean C57BL/6 mice and mitigate beneficial effects of weight loss on glucose homeostasis in obese mice. *Environ. Health Perspect.* **121**, 105–110.

Bennett, B. J., de Aguiar Vallim, T. Q., Wang, Z., Shih, D. M., Meng, Y., Gregory, J., Allayee, H., Lee, R., Graham, M., Crooke, R., *et al.* (2013). Trimethylamine-N-oxide, a metabolite associated with atherosclerosis, exhibits complex genetic and dietary regulation. *Cell Metab.* **17**, 49–60.

Brea, A., Mosquera, D., Martin, E., Arizti, A., Cordero, J. L., and Ros, E. (2005). Nonalcoholic fatty liver disease is associated with carotid atherosclerosis: A case-control study. *Arterioscler. Thromb. Vasc. Biol.* **25**, 1045–1050.

Carpenter, D. (2011). Exposure to polychlorinated biphenyls is associated with an increased risk of hypertension and cardiovascular disease. *Epidemiology* **22**, S147-S147. Meeting Abstract).

Chiappini, F., Coilly, A., Kadar, H., Gual, P., Tran, A., Desterke, C., Samuel, D., Duclos-Vallee, J. C., Touboul, D., Bertrand-Michel, J., *et al.* (2017). Metabolism dysregulation induces a specific

lipid signature of nonalcoholic steatohepatitis in patients. *Sci. Rep*. **7**, 46658.

Consonni, D., Sindaco, R., Agnello, L., Caporaso, N. E., Landi, M. T., Pesatori, A. C., and Bertazzi, P. A. (2012). Plasma levels of dioxins, furans, non-ortho-PCBs, and TEQs in the Seveso population 17 years after the accident. *Med. Lav*. **103**, 259–267.

Couper, K. N., Blount, D. G., and Riley, M. (2008). IL-10: The master regulator of Immunity to infection. *J. Immunol*. **180**, 5771–5777.

Getz, G. S., and Reardon, C. A. (2016). Do the Apoe-/- and Ldlr-/- Mice Yield the Same Insight on Atherogenesis? *Arterioscler. Thromb. Vasc. Biol*. **36**, 1734–1741.

Geusau, A., Abraham, K., Geissler, K., Sator, M. O., Stingl, G., and Tschachler, E. (2001). Severe 2, 3, 7, 8-tetrachlorodibenzo-p-dioxin (TCDD) intoxication: Clinical and laboratory effects. *Environ. Health Perspect*. **109**, 865–869.

Geyer, H. J., Scheunert, I., Rapp, K., Gebefugi, I., Steinberg, C., and Kettrup, A. (1993). The relevance of fat content in toxicity of lipophilic chemicals to terrestrial animals with special reference to dieldrin and 2, 3, 7, 8-tetrachlorodibenzo-p-dioxin (TCDD). *Ecotoxicol. Environ. Saf*. **26**, 45–60.

Goncharov, A., Bloom, M., Pavuk, M., Birman, I., and Carpenter, D. O. (2010). Blood pressure and hypertension in relation to levels of serum polychlorinated biphenyls in residents of Anniston, Alabama. *J. Hypertens*. **28**, 2053–2060.

Goncharov, A., Haase, R. F., Santiago-Rivera, A., Morse, G., McCaffrey, R. J., Rej, R., and Carpenter, D. O. (2008). High serum PCBs are associated with elevation of serum lipids and cardiovascular disease in a Native American population. *Environ. Res*. **106**, 226–239.

Guo, Y. L., Yu, M. L., Hsu, C. C., and Rogan, W. J. (1999). Chloracne, goiter, arthritis, and anemia after polychlorinated biphenyl poisoning: 14-year follow-Up of the Taiwan Yucheng cohort. *Environ. Health Perspect*. **107**, 715–719.

Han, S. G., Eum, S. Y., Toborek, M., Smart, E., and Hennig, B. (2010). Polychlorinated biphenyl-induced VCAM-1 expression is attenuated in aortic endothelial cells isolated from caveolin-1 deficient mice. *Toxicol. Appl. Pharmacol*. **246**, 74–82.

Hennig, B., Reiterer, G., Toborek, M., Matveev, S. V., Daugherty, A., Smart, E., and Robertson, L. W. (2004). Dietary fat interacts with PCBs to induce changes in lipid metabolism in mice deficient in low-density lipoprotein receptor. *Environ. Health Perspect*. **113**, 83–87.

Hong, N. S., Kim, K. S., Lee, I. K., Lind, P. M., Lind, L., Jacobs, D. R., and Lee, D. H. (2012). The association between obesity and mortality in the elderly differs by serum concentrations of persistent organic pollutants: A possible explanation for the obesity paradox. *Int. J. Obes*. **36**, 1170–1175.

Hopf, N. B., Ruder, A. M., and Succop, P. (2009). Background levels of polychlorinated biphenyls in the U.S. population. *Sci. Total Environ*. **407**, 6109–6119.

Kashima, S., Yorifuji, T., and Tsuda, T. (2011). Acute non-cancer mortality excess after polychlorinated biphenyls and polychlorinated dibenzofurans mixed exposure from contaminated rice oil: Yusho. *Sci. Total Environ*. **409**, 3288–3294.

Kim, S. A., Kim, K. S., Lee, Y. M., Jacobs, D. R., and Lee, D. H. (2015). Associations of organochlorine pesticides and polychlorinated biphenyls with total, cardiovascular, and cancer mortality in elders with differing fat mass. *Environ. Res*. **138**, 1–7.

Klaren, W. D., Flor, S., Gibson-Corley, K. N., Ludewig, G., and Robertson, L. W. (2016). Metallothionein's role in PCB 126 induced hepatotoxicity and hepatic micronutrient disruption. *Toxicol. Rep*. **3**, 21–28.

Kumar, J., Lind, P. M., Salihovic, S., van Bavel, B., Ingelsson, E., and Lind, L. (2014). Persistent organic pollutants and inflammatory markers in a cross-sectional study of elderly Swedish people: The PIVUS cohort. *Environ. Health Perspect*. **122**, 977–983.

La Merrill, M., Emond, C., Kim, M. J., Antignac, J. P., Le Bizec, B., Clement, K., Birnbaum, L. S., and Barouki, R. (2013). Toxicological function of adipose tissue: Focus on persistent organic pollutants. *Environ. Health Perspect*. **121**, 162–169.

Lassiter, R. R., and Hallam, T. G. (1990). Survival of the fattest: Implications for acute effects of lipophilic chemicals on aquatic populations. *Environ. Toxicol. Chem*. **9**, 585–595.

Lind, P. M., van Bavel, B., Salihovic, S., and Lind, L. (2011). Circulating levels of persistent organic pollutants (POPs) and carotid atherosclerosis in the elderly. *Environ. Health Perspect*. **120**, 38–43.

Lonardo, A., Sookoian, S., Chonchol, M., Loria, P., and Targher, G. (2013). Cardiovascular and systemic risk in nonalcoholic fatty liver disease - atherosclerosis as a major player in the natural course of NAFLD. *Curr. Pharm. Des*. **19**, 5177–5192.

Majkova, Z., Smart, E., Toborek, M., and Hennig, B. (2009). Up-regulation of endothelial monocyte chemoattractant protein-1 by coplanar PCB77 is caveolin-1-dependent. *Toxicol. Appl. Pharmacol*. **237**, 1–7.

Morck, A., Larsen, G., and Wehler, E. K. (2002). Covalent binding of PCB metabolites to lipids: Route of formation and characterization. *Xenobiotica* **32**, 625–640.

Mozos, I. (2015). Mechanisms linking red blood cell disorders and cardiovascular diseases. *Biomed. Res. Int*. **2015**, 682054.

Newsome, B. J., Petriello, M.C., Han, S.G., Murphy, M.O., Eske, K.E., Sunkara, M., and Hennig, B. (2014). Green tea diet decreases PCB 126-induced oxidatve stress in mice by upregulating antioxidant enzymes. *J Nutr Biochem*. **25**, 126–135.

Paigen, B., Morrow, A., Holmes, P. A., Mitchell, D., and Williams, R. A. (1987). Quantitative assessment of atherosclerotic lesions in mice. *Atherosclerosis* **68**, 231–240.

Petriello, M. C., Han, S. G., Newsome, B. J., and Hennig, B. (2014). PCB 126 toxicity is modulated by cross-talk between caveolae and Nrf2 signaling. *Toxicol. Appl. Pharmacol*. **277**, 192–199.

Schreinemachers, D. M., and Ghio, A. J. (2016). Effects of environmental pollutants on cellular iron homeostasis and ultimate links to human disease. *Environ. Health Insights* **10**, 35–43.

Sciullo, E. M., Vogel, C. F., Wu, D., Murakami, A., Ohigashi, H., and Matsumura, F. (2010). Effects of selected food phytochemicals in reducing the toxic actions of TCDD and p, p'-DDT in U937 macrophages. *Arch. Toxicol*. **84**, 957–966.

Serdar, B., LeBlanc, W. G., Norris, J. M., and Dickinson, L. M. (2014). Potential effects of polychlorinated biphenyls (PCBs) and selected organochlorine pesticides (OCPs) on immune cells and blood biochemistry measures: A cross-sectional assessment of the NHANES 2003-2004 data. *Environ. Health* **13**, 114.

Shan, Q., Wang, J., Huang, F., Lv, X., Ma, M., and Du, Y. (2014). Augmented atherogenesis in ApoE-null mice co-exposed to polychlorinated biphenyls and 2, 3, 7, 8-tetrachlorodibenzo-p-dioxin. *Toxicol. Appl. Pharmacol*. **276**, 136–146.

Silverstone, A. E., Rosenbaum, P. F., Weinstock, R. S., Bartell, S. M., Foushee, H. R., Shelton, C., and Pavuk, M. (2012). Polychlorinated biphenyl (PCB) exposure and diabetes: Results from the Anniston Community Health Survey. *Environ. Health Perspect*. **120**, 727–732.

Smith, D., and Lynam, K. (2012). GC/μECD analysis and confirmation of PCBs in fish tissue with agilent j&w db-35ms and db-xlb gc columns. *Agilent Application Note Food Anal*. 1–10. Available at: https://www.agilent.com/cs/library/applications/5990-6236EN.pdf, last accessed December 11, 2017.

Song, C., Burgess, S., Eicher, J. D., O'Donnell, C. J., and Johnson, A. D. (2017). Causal effect of plasminogen activator inhibitor type 1 on coronary heart disease. *J. Am. Heart Assoc.* **6**, e004918.

Tandra, S., Yeh, M. M., Brunt, E. M., Vuppalanchi, R., Cummings, O. W., Unalp-Arida, A., Wilson, L. A., and Chalasani, N. (2011). Presence and significance of microvesicular steatosis in nonalcoholic fatty liver disease. *J. Hepatol.* **55**, 654–659.

Teupser, D., Persky, A. D., and Breslow, J. L. (2003). Induction of atherosclerosis by low-fat, semisynthetic diets in LDL receptor-deficient C57BL/6J and FVB/NJ mice: Comparison of lesions of the aortic root, brachiocephalic artery, and whole aorta (en face measurement). *Arterioscler. Thromb. Vasc. Biol.* **23**, 1907–1913.

Tuomisto, J. T., Pohjanvirta, R., Unkila, M., and Tuomisto, J. (1999). TCDD-induced anorexia and wasting syndrome in rats: Effects of diet-induced obesity and nutrition. *Pharmacol. Biochem. Behav*. **62**, 735–742.

Uemura, H. (2012). Associations of exposure to dioxins and polychlorinated biphenyls with diabetes: Based on epidemiological findings]. Nihon. Eiseigaku Zasshi. *Japan. J. Hyg.* **67**, 363–374.

Wahlang, B., Perkins, J. T., Petriello, M. C., Hoffman, J. B., Stromberg, A. J., and Hennig, B. (2017). A compromised liver alters polychlorinated biphenyl-mediated toxicity. *Toxicology* **380**, 11–22.

Wang, Y., Chen, H., Wang, N., Guo, H., Fu, Y., Xue, S., Ai, A., Lyu, Q., and Kuang, Y. (2015). Combined 17beta-estradiol with TCDD promotes M2 polarization of macrophages in the endometriotic milieu with aid of the interaction between endometrial stromal cells and macrophages. *PloS One* **10**, e0125559.

Wu, D., Nishimura, N., Kuo, V., Fiehn, O., Shahbaz, S., Van Winkle, L., Matsumura, F., and Vogel, C. F. (2011). Activation of aryl hydrocarbon receptor induces vascular inflammation and promotes atherosclerosis in apolipoprotein E-/- mice. *Arterioscler. Thromb. Vasc. Biol.* **31**, 1260–1267.

Xu, P., Lou, X., Ding, G., Shen, H., Wu, L., Chen, Z., Han, J., and Wang, X. (2015). Effects of PCBs and PBDEs on thyroid hormone, lymphocyte proliferation, hematology and kidney injury markers in residents of an e-waste dismantling area in Zhejiang, China. *Sci. Total Environ.* **536**, 215–222.

Xu, S., Jay, A., Brunaldi, K., Huang, N., and Hamilton, J. A. (2013). CD36 enhances fatty acid uptake by increasing the rate of intracellular esterification but not transport across the plasma membrane. *Biochemistry* **52**, 7254–7261.

Zadelaar, S., Kleemann, R., Verschuren, L., de Vries-Van der Weij, J., van der Hoorn, J., Princen, H. M., and Kooistra, T. (2007). Mouse models for atherosclerosis and pharmaceutical modifiers. *Arterioscler. Thromb. Vasc. Biol.* **27**, 1706–1721.